Meas. Sci. Technol. 6 (1995) 1329–1337. Printed in the UK

An accurate non-contacting laser based system for surface wave velocity measurement

M G Somekh, M Liu, H P Ho and C W See

Department of Electrical and Electronic Engineering, University of Nottingham, University Park, Nottingham NG7 2RD, UK

Received 9 January 1995, in final form 6 June 1995, accepted for publication 16 June 1995

Abstract. This paper describes the development of a new optical system for accurate measurement of surface wave velocity and attenuation. A mode-locked *Q*-switch laser generates a Rayleigh wave tone burst which is detected with a two beam interferometer system. The resulting signals are then processed using a simple cross correlation algorithm. Results demonstrating the velocity resolution of the system are presented on both ceramic and metallic samples.

1. Introduction

There is an important need to measure surface acoustic wave (SAW) velocity at frequencies close to or above 100 MHz. At this frequency the wavelength is approximately 50 μm in ceramic materials and 30 μm in metals. The penetration depth of the surface wave is also comparable to the wavelength, so that measurements involving surface and near subsurface features require high operating frequencies in order to ensure that there is a strong interaction between the acoustic wave and the measurand. One obvious example where higher frequencies give a more useful measurement is in the determination of thin film thickness. In this situation it is necessary for the surface wave to interact with both the substrate and the coating so that the resultant velocity varies strongly with layer thickness. Clearly at lower frequencies the majority of the energy is concentrated in the substrate with the result that the wave velocity is insensitive to variations in the layer. For the same reason high frequencies are necessary for the determination of interface conditions between layer and substrate. Another important application is for the non-contacting determination of surface stress where the surface region of a material will be under stress which results in a small change in ultrasonic velocity. For ceramic materials such stressed regions can extend as little as a few micrometres, requiring surface wave measurements at, ideally, several hundred MHz.

The scanning acoustic microscope [1], operating in the so-called $V(z)$ mode, is used effectively for surface wave velocity measurements between 50 and 400 MHz. The problem with this technique lies principally in the fluid couplant, which can make access to some samples problematic. In addition the fluid couplant loads the surface wave causing it to attenuate continuously into the couplant. This greatly reduces the propagation distance of the wave, thus degrading the accuracy and also makes the signal processing procedure somewhat arbitrary. A further disadvantage of the $V(z)$ method is the requirement to move the sample mechanically in order to alter the sample/lens spacing. There is therefore considerable advantage to be gained in developing a non-contacting technique capable of accurate surface wave measurement at high frequencies. Laser ultrasonics is the obvious candidate for this task [2–6]. This paper discusses the development of such a system which is capable of accurate surface wave measurement, which removes the need for mechanical movement, largely eliminates the problems of timing jitter and can routinely and rapidly produce surface wave measurements with comparable (and ultimately better) accuracy than the scanning acoustic microscope.

The motivation for the development was to produce an instrument capable of measuring small changes in SAW velocity with a view to assessing whether surface wave measurements alone were capable of detecting the stress state of various ceramic materials. The results described here show that the technique is indeed capable of detecting small changes in velocity induced by stress. Clearly the system can be applied to other applications requiring accurate surface wave velocity and attenuation measurements mentioned earlier in this section.

2. System design

2.1. Continuous wave versus pulsed generation

The first design issue to be resolved hinges on whether the system should operate with continuous ultrasonic waves or pulses. This decision not only affects the generation

0957-0233/95/091329+09$19.50

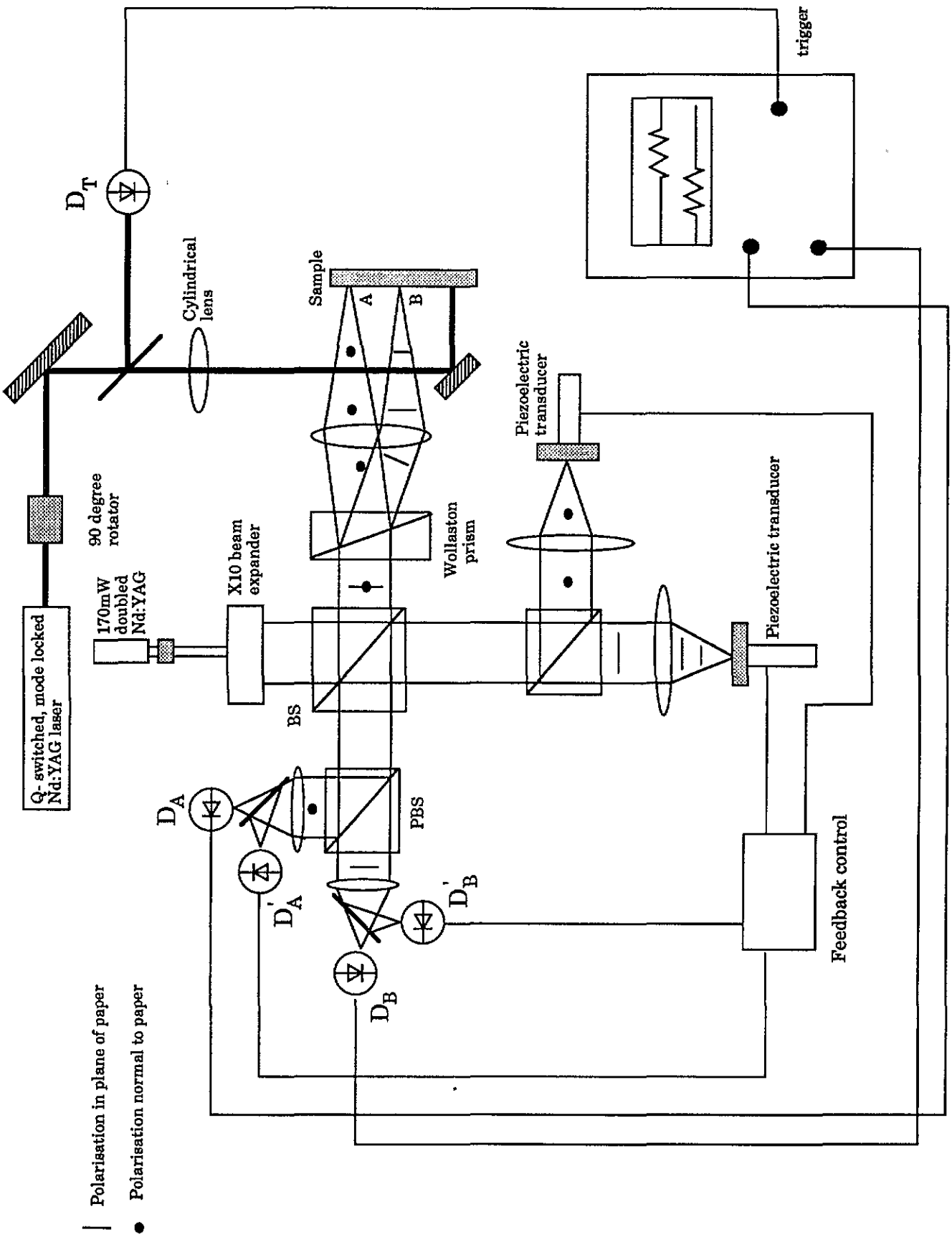

Figure 1. Schematic diagram showing both SAW detection and generation configurations of the dual beam optical surface wave measurement system.

system but also the detection. In order to generate measurable surface wave amplitudes a continuous wave system requires a large average optical power compared with a pulsed system, because the amplitude of the laser generated ultrasonic signal is proportional to the optical power. This will result in considerable background (DC) heating on the sample. On the other hand, in order to recover an accurate velocity measurement from a single pulsed measurement it is necessary to extract the component in a very narrow band. This means that only a small fraction of the energy is used in the measurement. This problem becomes increasingly severe as the frequency is increased, since the lower ultrasonic frequencies are excited more efficiently than higher frequencies. The peak optical powers on the surface are therefore very high, so although the DC heating is manageable, damage can result from a high powered single pulse ([4] p 423). The approach taken in this paper uses a Q-switch mode locked laser pulse, which sends out a pulse train with a well defined repetition frequency, this system combines advantages of both continuous wave and pulsed systems.

2.2. Generation system

Figure 1 shows a schematic diagram of the system used for ultrasonic generation and detection. The generation is performed using a mode-locked Q-switched laser which produces a burst of approximately thirty pulses whose duration is approximately 400 ps and whose separation is 12.2 ns. The light from the laser is focussed onto the sample by a cylindrical lens, the illumination on the sample surface is thus a line of length approximately 5 mm and width 15 μm. The output from the laser gives rise to a burst of surface acoustic waves whose fundamental frequency is 82 MHz. A trace of the output from the generating laser is shown in figure 2. In this paper results are obtained at the fundamental frequency only, although with appropriate electrons single frequency operation at harmonics of this frequency could be readily achieved.

2.3. Interferometer detection system

The main difference between the present interferometer and the system described in [7] is that the system used here is homodyne whereas the system described before was a heterodyne interferometer. This means that the output signal from one arm can be expressed as:

$$i(\theta) = |R|^2 + |S|^2 + 2|R||S|\cos\theta \qquad (1)$$

where $i(\theta)$ is the output current as a function of the phase difference between the reference arm and the sample arm. $|S|$ and $|R|$ represent the modulus of the reflected fields arriving from the sample and reference arms respectively. From equation (1) it can be seen that the output signal varies sinusoidally. When an interferometer is used for detection of rapidly varying surface waves the phase difference, θ, between the two signals can be expressed as:

$$\theta = 2k(z_0 + \Delta z \cos\omega_m t) \qquad (2)$$

where k is the wavenumber of the interferometer illumination, z_0 is the static path difference between the reference and signal arms, Δz is the displacement of the surface wave oscillating at frequency ω_m. For the practical amplitudes of interest Δz is considerably smaller than the optical wavelength, and it can be readily seen that when $2kz_0$ (in equation (2)) is close to $n\pi$, where n is an integer, the sensitivity to the small AC vibrations becomes vanishingly small. On the other hand the best sensitivity to surface vibrations is obtained when $2kz_0$ is $(n + \frac{1}{2})\pi$, that is where the gradient of the sinusoidal variation with displacement is greatest. In order to ensure sensitive operation measurements need to close to the optimum sensitivity point.

The laser detection system shown in figure 1 consists of two interferometers in parallel, so that each arm independently detects the surface displacement under probes A and B respectively. The two-probe beam structure is well suited for accurate velocity measurement since each probe independently measures the phase of the surface wave passing under it. This allows one to compute the time delay, so that the velocity may be readily determined once the probe separation is known.

The laser source used in the present system is a dipole-pumped frequency-doubled YAG laser operating at 532 nm, giving 170 mW of output power. Although this high power is convenient we have achieved quite satisfactory operation with a 7 mW 633 nm HeNe laser. After passing through an optical isolater the light passes through the beamsplitter onto a Wollaston prism where the two orthogonal polarizations are split in angle so that they focus on adjacent points on the sample. These two beams are then reflected back through the system, with their polarizations so adjusted that beam A interferes with R_A and beam B interferes with R_B, whose outputs are detected at D_A and D_B respectively. The system thus operates as two interferometers in parallel, with a measured electrical crosstalk between the two arms of less than -70 dB.

In order to maintain the system operating at the position of greatest sensitivity a portion of the output signal from each arm is detected by detectors D'_A and D'_B respectively. The low-pass filtered output from each of these detectors is then fed into a comparator, which compares the output with a reference value so that deviations from the desired level are fed back to the respective piezo pusher, thus correcting the phase of the reference beam so that a fixed operating point for the system is maintained.

The output signals from detectors D_A and D_B contain a fixed level output resulting from the maintenance of the interferometers at the position of best sensitivity with the small perturbation superimposed, which arises when the surface acoustic wave passes under the corresponding probe beam. These signals are amplified and filtered prior to detection in two channels of a digital oscilloscope, which is triggered from the output of detector D_T which detects the output from the pump laser. The two channels of the digital scope thus allow one to compare the surface wave signal detected by each probe beam. The pump power levels on the sample are such that it is necessary to average the output signals. Figure 3(a) shows a typical trace obtained from one

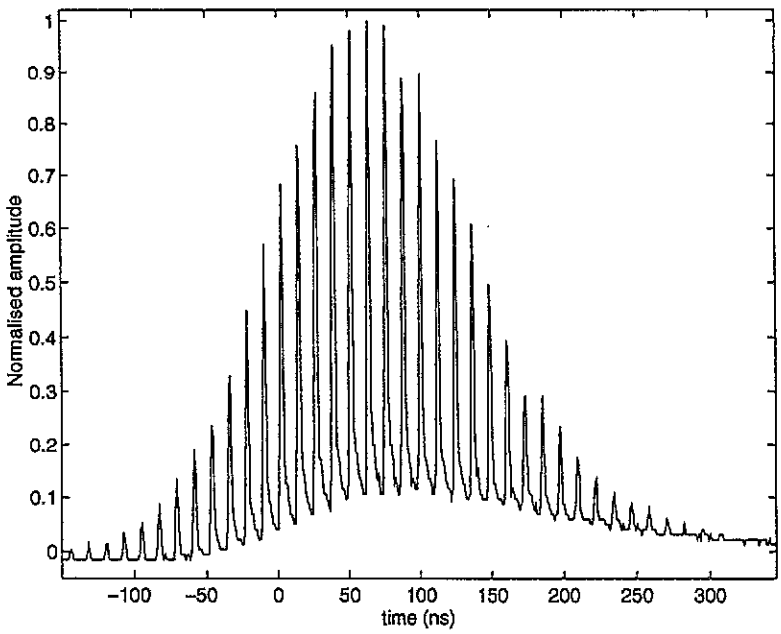

Figure 2. Oscilloscope trace showing optical 'tone burst' from *Q*-switched mode locked YAG laser.

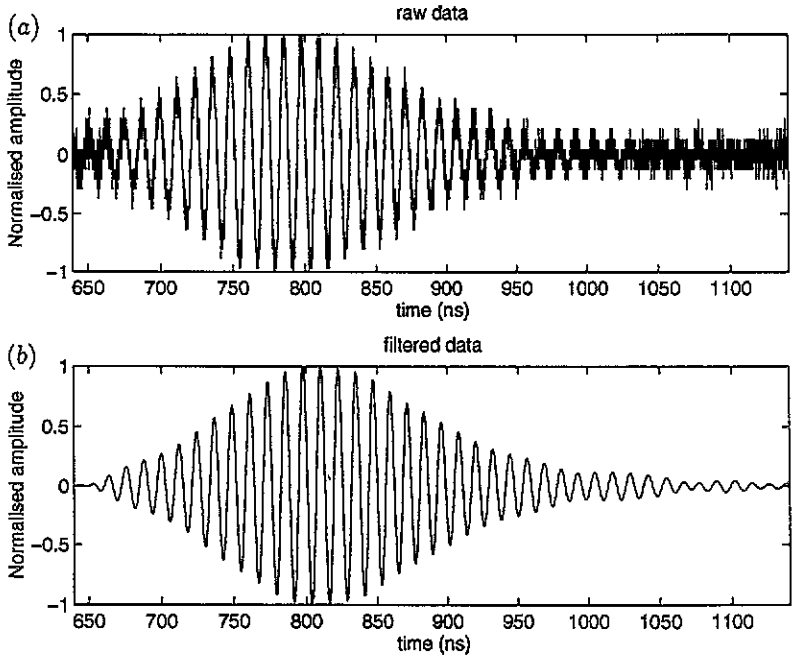

Figure 3. Surface wave signals detected by the optical detection interferometers. (*a*) Trace obtained under a single probe after averaging. (*b*) As (*a*) after passing through a digital filter with 10 MHz bandwidth.

probe beam on a silicon nitride sample after averaging the tone burst traces 500 times. After a measurement cycle the oscilloscope memory will typically contain two 5000 point traces digitized to bits corresponding to the surface waves passing under each probe. This data is then transferred to the personal computer for subsequent data processing.

2.4. Signal processing algorithm

For convenience, all the processing algorithms have been written using the software package MATLAB, which provides an efficient high level environment for analysing the signals. The two input signals are initially filtered with a narrowband digital filter, which greatly reduces the noise, facilitating viewing of the waveforms (although this is not strictly necessary for the processing because subsequent filtering applies an even narrower bandpass filter). Figure 3(*a*) shows the signal detected under one beam prior to filtering and figure 3(*b*) shows the effect of the 10 MHz band-pass filter. In order to obtain the time delay between the two beams their cross correlation

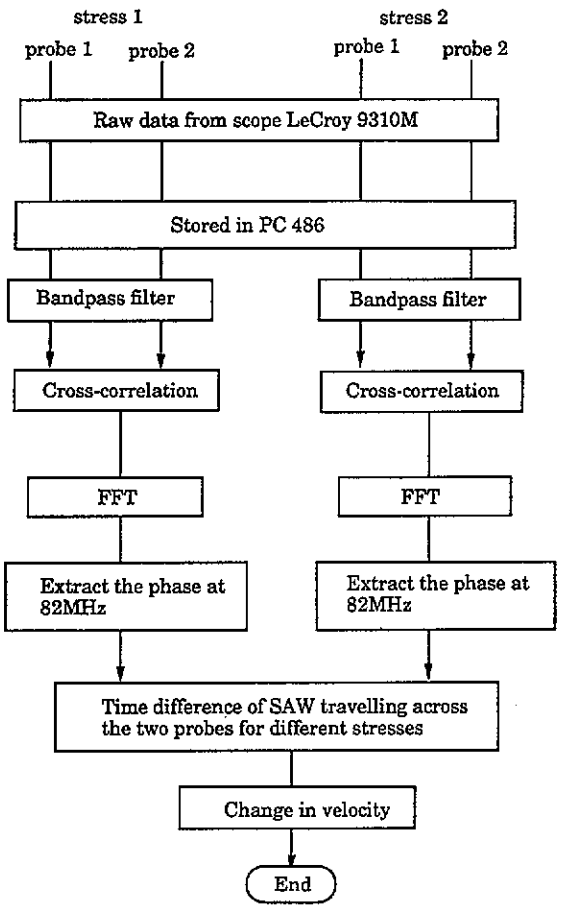

Figure 4. Algorithm showing extraction of surface wave velocity changes.

is obtained using the fast Fourier transform facility built into MATLAB. The phase of the cross-correlation signal at 82 MHz can then be readily used to extract the time delay between the two signals. It must be noted, however, that the phase so extracted is only known *modulo* 2π, so the approximate number of wavelengths must either be known or determined using an alternate method involving a calculation of the mean delay time from the envelope of the surface wave train. In the experiments reported here on silicon nitride with a beam separation of 1.1 mm, the mean delay corresponded to either 15 or 16 surface wavelengths.

The algorithm used to determine the velocity difference between the sample in different stress states is shown in figure 4. In order to appreciate the operation of the measurement process figure 5(*a*) shows the cross correlation between the output signals from each probe. Figure 5(*b*) shows a blow-up of the cross-correlation traces where the solid curve is derived from the signal in the unstressed state and the dashed curve shows the phase shifted curved when the same sample is subjected to a stress difference of 280 MPa, indicating a reduction in SAW velocity.

2.5. Errors and accuracy

It is necessary to give some consideration to the errors in the velocity measurement process, and also to distinguish between factors which affect the absolute measurement of SAW velocity and those which affect the measurement of the velocity changes.

The principal limitation in the measurement of absolute velocity is the accurate determination of the probe separation. This has been measured by scanning a knife edge across the two probes and determining the separation from the transition, this gives an uncertainty of approximately 1 part in 1000. This is acceptable since we

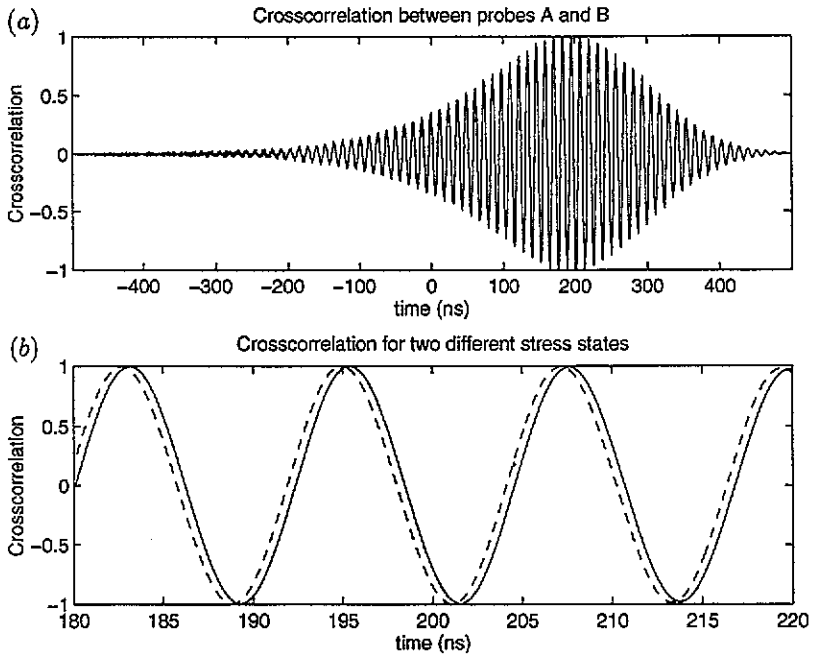

Figure 5. (*a*) The cross correlation obtained from the signal under probes A and B. (*b*) Expanded version of the cross-correlation trace of (*a*) (solid curve) with a phase shifted version arising from an increase in tensile stress on a steel sample of 280 MPa.

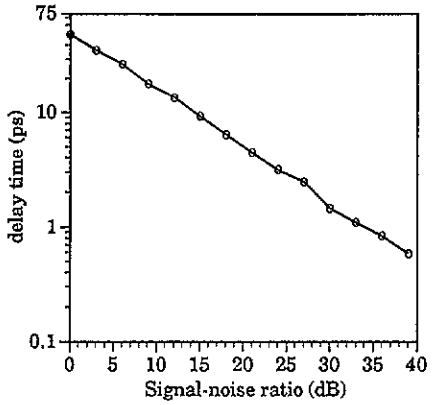

Figure 6. Calculated value of the timing uncertainty introduced by noise as a function of signal-to-noise ratio.

are concerned primarily with measuring changes in SAW velocity. If, however, we wished to further enhance the absolute accuracy a fringe counting interferometer can be attached to the scan stage.

For our applications relative changes in velocity are of far more importance than absolute velocity measurement. We now discuss factors that lead to uncertainties in the relative velocity measurement. These relate to the possible errors in the timing between the two probes. One instrumental source of such an error is the jitter inherent in the digital oscilloscope. This was tested by inputting two identical (noiseless) 82 MHz sinusoidal signals into each channel of the digital oscilloscope and measuring the apparent delay over a series of measurements. The RMS value of this uncertainty was found to be approximately 3 ps.

One fundamental source of error whose ultimate limit is set by the signal-to-noise ratio of the SAW detection process. In order to relate the timing error to the input

Table 1. SAW velocity variation with temperature drift.

Temperature during measurement (K)	SAW velocity ($m\ s^{-1}$)	Remarks
24.9–25.4	5675.3	Heaters are
26.3–26.4	5678.6	used to increase
27.9–28.2	5672.3	the room
28.9–29.1	5668.3	temperature
26.0–26.3	5671.4	no heaters
25.7–26.4	5671.6	
25.9–26.3	5670.6	
25.7–26.0	5671.6	

signal-to-noise ratio, a series of computer simulations were performed. A tone burst with a Guassian envelope was added to randomly generated noise so that the input signal-to-noise ratio could be varied. The signal-to-noise ratio of the input signal was well defined in the following manner:

$$SNR = 10 \log_{10} \frac{P_{sig}}{\sigma^2} \tag{3}$$

where P_{sig} is the signal power, and σ^2 is the variance of the Gaussian noise.

The resulting signals plus noise were then passed through the processing algorithm described in section 2.4 so that the variation in the measured delay between the two signals could be calculated. This process was repeated for each signal-to-noise ratio using different sets of randomly generated noise. The timing uncertainty as a function of input signal-to-noise ratio is plotted in figure 6, where it can be seen that the processing algorithm is very robust in its resistance to noise. In order to compare the quality of the actual input signal with the various simulated values of signal-to-noise ratio, figure 7 compares an experimental waveform with a measured *SNR* of 12.5 dB (figure 7(*a*))

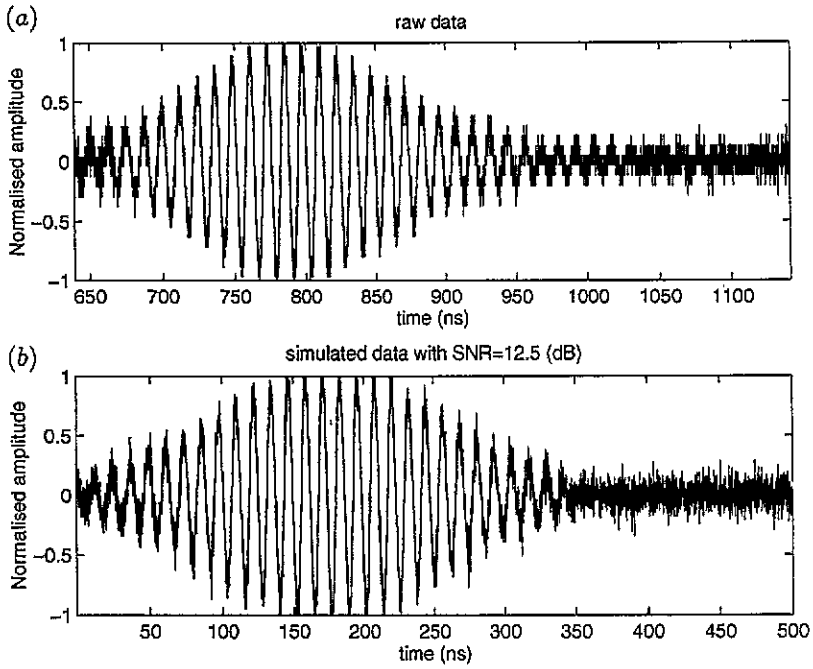

Figure 7. Comparison of experimental and simulated surface wave traces with *SNR*s of 12.5 dB. (*a*) Experimental trace. (*b*) Simulated trace.

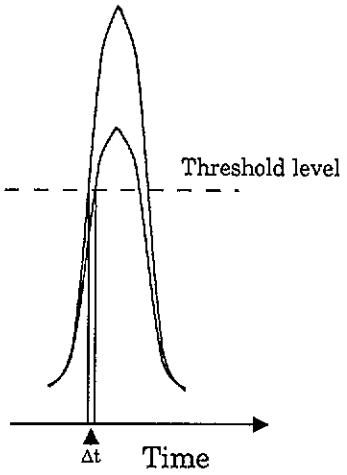

Figure 8. Schematic diagram showing how a timing error arises from pulse jitter.

and simulated waveform with a similar *SNR* (figure 7(*b*)). It can be seen that then two signals have comparable *SNR*. From figure 6 we see that an *SNR* of 12.5 dB imposes an RMS error in the measured delay of 8 ps. It should be noted that random interleaving is used in the digital oscilloscope, so that two adjacent noise signals may be uncorrelated because they are actually derived from signals well separated in time. The noise bandwidth thus corresponds more closely to the sampling interval rather than the analogue bandwidth of the detection.

Another possible source of error that was identified related to the variation in the output power of the laser between pulses. This means that setting the trigger to a fixed level translates to timing jitter, because the time that a pulse takes to reach a particular level is determined by the ultimate height of the pulse (see figure 8). If the time between excitation of the pulse and detection by a single pulse was used this would be a very severe source of error. In the two beam configuration we use here this effect is largely eliminated because the system measures the time delay between the probes so that timing jitter due to amplitude fluctuations is common to each beam. To a large extent this accounts for the very good accuracy obtained with our system compared to single beam systems.

Another source of error relates to the variation in ambient temperature. Clearly temperature variation affects the actual sound velocity of the wave propagating through the sample (by typically 1 m s^{-1} per degree K), moreover the change in temperature will alter the separation of the probes. Reliable measurements are thus clearly achieved when the temperature is stabilised. Table 1 gives measured velocities on a sample of silicon nitride as the ambient temperature is varied. The results indicate the excellent stability of the system when the temperature is stable.

If the temperature is stabilized and the jitter errors are uncorrelated we may expect an RMS timing error of $\approx$ 8.5 ps. For a beam separation of 1.1 mm this corresponds to an uncertainty in relative velocity for silicon nitride with a nominal SAW velocity of 5800 m s^{-1} of approximately 0.26 m s^{-1} or one part in 20 000. The results in table 1 indicate that under stable temperature conditions such values may be achieved.

This value compares favourably with those quoted for contact methods such as line focus acoustic microscopy [1]. Comparisons between velocity measurements on the sample measured with the scanning acoustic microscope show that velocity measurements on the same sample differ by, on average, less than one part in 10^3. These results are tabulated in table 2†.

Table 2. SAW velocity measured by the system and acoustic microscope.

Sample	Measured SAW velocity (m s^{-1})	Acoustic microscope measurement (m s^{-1})
Sample 1	5524.2	5522.7
Sample 2	5543.1	5543.9
Sample 3	5797.1	5783.9
Sample 4	5773.5	5763.5

3. Results

In order to demonstrate the effectiveness of the system for velocity measurements we present results that show the variation of velocity with applied stress. It is well known

† The comparative measurements on the line focus acoustic microscope were made at the Department of Materials, University of Oxford, whose assistance we gratefully acknowledge.

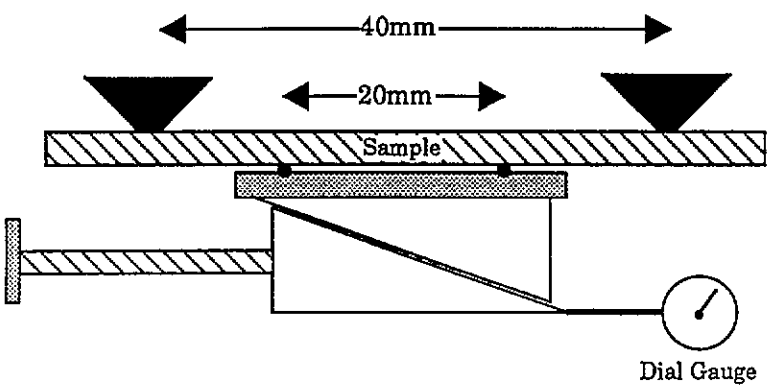

Figure 9. Schematic diagram of four-point bending jig, showing critical dimensions.

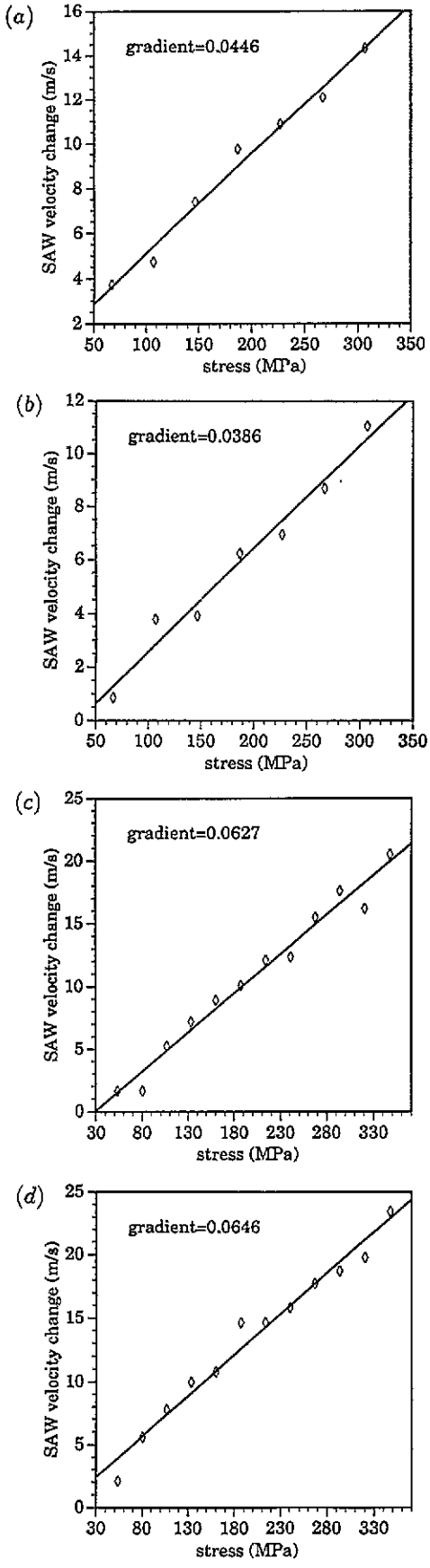

Figure 10. Experimental curves showing variation in SAW velocity on samples of silicon nitride with applied tensile stress. (*a*) Location 1, sample 1, Norton hot pressed silicon nitride. (*b*) Location 2, sample1, Norton hot pressed silicon nitride. (*c*) Location 1, sample 2, Norton hot pressed silicon nitride. (*d*) Location 2, sample 2, Norton hot pressed silicon nitride.

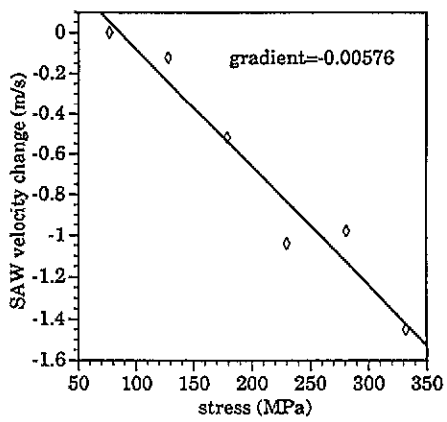

Figure 11. Experimental curve showing variation in SAW velocity on steel sample versus applied tensile stress.

that the third-order elastic constants determine the changes in the sound velocity with applied stress. The changes in velocity are small, typically of the order of one part in 10^3 or less. Naturally, such measurements require an accurate measurement of velocity change. The experiments described below have been carried out in order to determine whether the non-contacting surface wave system can be used to determine the stress state of materials. In order to do this successfully we impose a well calibrated external stress in order to determine whether the velocity changes can be measured.

The samples were cut into bars of dimensions, $50 \times 5 \times 3$ mm so that they could fit into a four-point bending jig whose operation and dimensions are shown schematically in figure 9. The mechanical bending jig was calibrated using a strain gauge onto a steel sample. All the settings of the strain gauge as well as the dial gauge were recorded and then used to calculate the bending stresses according the four point bending equation. For other materials the stress applied was deduced from the reading of the dial gauge by setting the linear relationship to a corresponding Young's modulus.

The samples were placed in the stressing jig and the time delay under each beam was recorded in the digital oscilloscope. The algorithm described in section 2.4 was then used to recover the surface wave velocity. The samples were then subjected to a varying stress and the velocity changes were recorded. The imposition of a stress level deformed the sample slightly so it was necessary to reposition the sample using a travelling microscope mounted over the stressing jig. This allowed the accurate realignment of the sample to better than one micrometer. It should be mentioned, however, that a stressing jig in which the centre of the sample was kept stationary would facilitate more rapid measurements.

Figures 10(*a*)–(*d*) show the variation in velocity with applied stress on various silicon nitride samples. These indicate that the system is indeed capable of measuring the small changes in velocity imposed by applied stress. The results show the velocity increasing with applied tensile stress with a mean change of 0.038–0.064 m s^{-1} MPa^{-1}. This shows a similar trend to the results described in [8] where the SAW velocity also increased with stress, although

the velocity change we observe is much smaller. The results shown in figure 11 on the steel samples show the SAW wave velocity decreasing with applied tensile stress consistent with the results in the literature [9].

The measurements on silicon nitride appear to have slightly more scatter than those on steel. This is due in part to the non-uniformity of the sample and also to the fact that the lower SAW velocity on steel means that a given phase error corresponds to a smaller velocity change. It is worth pointing out that SAW measurements on the scanning acoustic microscope are poorer for fast materials than slower ones because of the difficulty of obtaining a sufficient number of interference fringes in the $V(z)$ curve.

4. Summary and future developements

This paper describes the developement of an optical system for non-contacting measurement of surface wave velocity. We show that the two beam system is very suitable for accurate measurements being largely immune to the effect of timing jitter due to laser power fluctuations. In its present implementation the system appears capable of relative SAW measurements to one part in 10^4. Further improvements in the temperature stabilisation will result in still greater improvements.

In order to use the system for the measurement of residual stress in ceramics, it would be beneficial to operate at a higher modulation frequency. This can be achieved by filtering the electrical output at harmonic of the modulation frequency and further improvements in the frequency selectivity can be achieved by using grating excitation to enhance the high frequencies at the expense of the lower ones.

Acknowledgements

We gratefully acknowledge support from the CEC under BRITE EURAM (project no BE 4398), Rolls Royce PLC and The Royal Society. We wish also to thank our partners particularly IWT Bremen, for construction and calibration of the stressing jig, and SKF Engineering Research Centre BV, Netherlands for provision of the majority of the samples examined.

References

[1] Kushibiki J and Chubachi N 1985 Material characterisation by line focus beam acoustic microscope *IEEE Trans. Sonics Ultrasonics* **32** 189

[2] Aussel J-D and Monchalin J-P 1989 Precision laser-ultrasonic velocity measurement and elastic constant determination *Ultrasonics* **27** 165

[3] Huang J and Achenbach J D 1991 Dual probe laser interferometer *J. Acoust. Soc. Am.* **90** 1269

[4] Scruby C B and Drain L E 1991 *Laser Ultrasonics: Techniques and Applications* (Bristol: Adam Hilger)

[5] Noui L and Dewhurst R J 1993 A laser-beam deflection technique for the quantative detection of ultrasonic lamb waves *Ultrasonics* **31** 425

[6] Karabutov A A 1985 Laser excitation of surface acoustic waves: a new direction in opto-acoustic spectroscopy of solids *Sov. Phys.–Usp.* **28** 1042

[7] Ho H P, Somekh M G, Liu M and See C W 1994 Direct and indirect dual-probe interferometers for accurate surface wave measurements *Meas. Sci. Technol.* **5** 1480

[8] Tanaka S and Miyasaka C 1992 Residual stress distribution in a ceramic/metal joint evaluated from the $V(z)$ curves of a scanning acoustic microscope *Residual Stresses III: Science and Technology* vols 1&2, ed H Fujiwara *et al* (Amsterdam: Elsevier)

[9] Hirao M, Fukuoka H and Horii K 1981 Acoustic effect of Rayleigh surface-wave in isotropic material *J. App. Mech.* **48** 119